



Cite this: *RSC Adv.*, 2024, **14**, 18330

## Antioxidant activity of an inclusion complex between rutin and $\beta$ -cyclodextrin: experimental and quantum chemical studies

Thi Lan Pham, <sup>\*ab</sup> Thi Thu Ha Nguyen, <sup>c</sup> Tuan Anh Nguyen, <sup>a</sup> Irina Le-Deygen, <sup>d</sup> Thi My Hanh Le, <sup>a</sup> Xuan Minh Vu, <sup>a</sup> Hai Khoa Le, <sup>a</sup> Cuong Bui Van, <sup>a</sup> T. R. Usacheva, <sup>e</sup> Thanh Tung Mai <sup>f</sup> and Dai Lam Tran <sup>a</sup>

This study aims to synthesize a guest–host complex derived from rutin (Rut) and  $\beta$ -cyclodextrin ( $\beta$ -CD) (denoted as  $[\text{Rut} \subset \beta\text{-CD}]$ ). The obtained substance was characterized by the FT-IR and DSC methods, signifying the formation of an inclusion complex between Rut and  $\beta$ -CD. Complex formation increased the antioxidant activity of rutin corresponding to the decrease of  $\text{EC}_{50}$  values from  $1.547 \times 10^{-5}$  mol L<sup>-1</sup> to  $1.227 \times 10^{-5}$  mol L<sup>-1</sup> according to the DPPH free radical scavenging test. The rutin- $\beta$ -CD interaction energies were calculated in the vacuum and various solvents (e.g., water, ethanol, and dimethylsulfoxide) utilizing an accurate and broadly parametrized self-consistent tight-binding quantum chemical method (GFN2-xTB). The calculation results reveal the influence of solvent on the structural formation of the rutin- $\beta$ -CD complex. In both the vacuum and aqueous solution, rutin can enter into the small-sized empty cavity of  $\beta$ -CD, albeit through different terminals, resulting in distinct preferential structures. The presence of organic solvents appears to reduce the interaction between rutin and  $\beta$ -CD, with the interaction strength following the order: water > ethanol > dimethyl sulfoxide.

Received 26th March 2024  
 Accepted 3rd June 2024

DOI: 10.1039/d4ra02307b  
[rsc.li/rsc-advances](http://rsc.li/rsc-advances)

## 1 Introduction

Drugs generated from natural compounds are of increasing interest because of their powerful therapeutic potential and minimal adverse effects. Flavonoid-based compounds found in many plants have strong biological activity, making them some of the most promising classes of pharmaceuticals.<sup>1</sup> Because of the ability to regulate immunological responses, viruses, and carcinogens, flavonoids have been labeled “nature’s biochemical repairmen”. Flavonoid compounds have considerable antioxidant activity due to unique features in their chemical structure: (i) hydroxyl groups that bind to aromatic rings can give hydro atoms, and (ii) aromatic rings (e.g., benzene rings, hetero-element rings) and double bonds (e.g., C=C and C=O bonds) create a conjugated system, stabilizing free radicals.

Rutin (quercetin-3-rutinoside, Rut), is a flavonol glycoside composed of the flavonol quercetin and the disaccharide rutinose.<sup>2</sup> Rutin, a well-known bioflavonoid, is found abundantly in many natural plants such as tea, some fruits, buckwheat, etc. In particular, the flower buds of *Sophora japonica* L. contain high levels of rutin, which have great opportunities for use in the pharmaceutical production.<sup>3</sup>

The antioxidants, containing rutin in the structural backbone, have proven precious biological activities.<sup>4,5</sup> For instance, rutin has been found to resist various viruses (e.g., H5N1, HSV, dengue, HIV and SARS-CoV-2) suggesting the potential application of this compound in the biomedical field.<sup>6–8</sup> However, the extremely low water solubility of rutin requires a large intake, which can induce high toxicity at low bioavailability.

Numerous investigations have attempted to address the mentioned issues. To this end, cyclodextrin (CD) has been recognized as the outstanding capability to improve the solubility and bioavailability through rutin-cyclodextrins complexes.<sup>9–15</sup> Heretofore, the complex has been synthesized *via* various methods (e.g., co-precipitation, wet grinding, kneading) and exhibited significant enhancement of rutin’s solubility.<sup>10–12,15</sup> It has been found that the direct hydroxyl groups-aromatic ring linkage, which is capable of donating hydrogen atoms, promotes the capture of free radicals.<sup>13,14</sup> Min Liu and colleagues suggested that the increase of quercetin antioxidant activity in complexes with the three cyclodextrin derivatives was due to the enhancement of hydrogen donation capacity after complexation.<sup>13</sup> Thus, as-generated

<sup>a</sup>Institute for Tropical Technology, Vietnam Academy of Science and Technology, 18 Hoang Quoc Viet, Cau Giay, Hanoi, Vietnam. E-mail: ptlan@itt.vast.vn

<sup>b</sup>Graduate University of Science and Technology, Vietnam Academy of Science and Technology, 18 Hoang Quoc Viet, Cau Giay, Hanoi, Vietnam

<sup>c</sup>Hanoi National University of Education, 136 Xuan Thuy, Cau Giay, Vietnam

<sup>d</sup>Chemical enzymology department, Lomonosov Moscow State University, Leninskie gory 11b, Moscow, Russian Federation

<sup>e</sup>Ivanovo State University of Chemistry and Technology, Sheremetevsky Avenue 7, 153000 Ivanovo, Russian Federation

<sup>f</sup>Hanoi University of Science and Technology, 1 Dai Co Viet, Bach Khoa, Hai Ba Trung, Hanoi, Vietnam



intermolecular hydrogen bonds weaken intramolecular hydrogen bonds of quercetin, leading to improve the hydrogen donation capability of quercetin. However, the antioxidant activity of the rutin-cyclodextrin complex has been controversial. Currently, a disagreement about the antioxidant activity of the rutin-cyclodextrin complex has emerged. Some studies suggested that after complexation, the antioxidant capacity of rutin increased significantly,<sup>10,16</sup> whereas others showed a decrease or almost no change in the complex's activity compared to pure rutin.<sup>14</sup> Therefore, the mechanism of complex formation and the binding centers of the two molecules should be revealed. More importantly, the aim of this work is to study the role of the phenolic hydroxyl functional groups of rutin in complex formation.

Recent researches have attempted to address the structure and complexation mechanism of rutin and some flavonoids. Hydrogen bondings formed between the oxygen atoms of cyclodextrin and the hydrogen atoms of rutin forms inclusion complexation have been explored.<sup>11,17,18</sup> Our previous works demonstrated, that complexing the A-ring (double ring) of rutin molecules, it penetrated into the cavity of 2-hydroxypropyl- $\beta$ -cyclodextrin (HP- $\beta$ -CD) molecule in the direction of the larger bottom.<sup>18</sup> The presence of the hydroxylpropyl functional groups significantly affected the structure of CD. One side of the HP- $\beta$ -CD molecule was significantly enlarged in comparison to the  $\beta$ -CD molecule. Such expansion facilitates the complete penetration of the A-ring of the molecule into the cavity of HP- $\beta$ -CD. However, a question has emerged that which part of the rutin molecule will preferentially "enter" into the hollow cavity of the  $\beta$ -CD molecule and in which direction, if a hydroxylpropyl group at the outer edge of the host molecule is absent?

Our previous experimental studies on the effect of the reaction medium (vacuum or solution, water or organic solvent) on the complexation reaction [Rut $\subset$ HP- $\beta$ -CD] found that the interaction of rutin with HP $\beta$ CD in water was stronger than in ethanol.<sup>12,19</sup> The results were confirmed by theoretical calculation.<sup>19</sup> Moreover, the calculation results of HOMO and LUMO also showed that there was a clear difference in the two vacuum and water environments.<sup>19</sup> In a vacuum, HOMO was distributed mainly on the host molecule (HP $\beta$ CD), while LUMO was completely concentrated on the guest molecule (Rut). However, in water, both HOMO and LUMO of the complex were contributed mainly by rutin. Thus, in the water, the interaction between rutin and HP $\beta$ CD was significantly reduced compared to those in vacuum. The effect of mixed solvents on the thermodynamics of complexation between rutin and cyclodextrin was also studied.<sup>12,19</sup> The results indicated that the stability of the complexes gradually decreased with the increasing ethanol concentration in solvent. At the same time, the enthalpy of the reaction markedly decreased with the increasing organic component in the mixed solvent. Thus, the nature of the reaction environment has a great influence on the ability of cyclodextrin to interact with rutin as well as the thermodynamics of the complexation reaction. Therefore, to continue our studies on rutin-cyclodextrin complex, here the complex of rutin and  $\beta$ -cyclodextrin ([Rut $\subset$  $\beta$ -CD]) has been synthesized, characterized and evaluated the antioxidant activity. A theoretical chemical calculation method has been conducted to identify the binding center of  $\beta$ -cyclodextrin with rutin in different environments:

vacuum, water, ethanol (polar protic solvent) and dimethylsulfoxide (polar aprotic solvent). Then, the effect of the hydroxylpropyl functional group on the complexation ([Rut $\subset$ HP- $\beta$ -CD])<sup>19</sup> was also compared with the complexation ([Rut $\subset$  $\beta$ -CD]) in the absence of the hydroxylpropyl group at the edge of the host molecule. In addition, the antioxidant ability of rutin before and after complexation with  $\beta$ -cyclodextrin in different solvents has been evaluated and confirmed through theoretical calculations.

## 2 Experimental

### 2.1. Preparation of inclusion complex

The complex of Rut and  $\beta$ -CD was synthesized in mixed EtOH-H<sub>2</sub>O (20 : 80, v/v) solvent according to the follow steps: briefly, the  $\beta$ -CD solution ( $5 \times 10^{-3}$  M) was added into rutin solution ( $5 \times 10^{-3}$  M) and stirred for 24 h at 25 °C. Afterwards, the mixture was kept for 48 hours at 4 °C to produce a fine yellow precipitate. The as-prepared product was washed with DMSO (10 mL, 3 times) and freeze-dried for 48 hours to obtain the product in dry form.

### 2.2. Characterization

**2.2.1. FTIR.** The [Rut $\subset$  $\beta$ -CD] complex powder was structurally analyzed using Fourier transform infrared spectroscopy (FTIR) (Nicolet Nexus 670) using KBr tablets. Rut and  $\beta$ -CD were also analyzed simultaneously for comparison. In the mixture with KBr, the contents of RuT,  $\beta$ -CD and complex samples were all equal to 5% wt.

The [Rut $\subset$  $\beta$ -CD] complex aqueous solution was analyzed using ATR-Fourier transform infrared spectroscopy (ATR-FTIR). Spectra were obtained from Bruker Tensor 27 ATR-FTIR Fourier spectrometer equipped with an MCT detector cooled with liquid N<sub>2</sub> and a Huber thermostat. The measurements were carried out in a BioATR II thermostated cell using a single reflection ZnSe element at 22 °C and continuous purging of the system with dry air using a compressor. In a typical experiment the volume of the sample was 50  $\mu$ L and the spectra were recorded three times in the range from 3000 to 950  $\text{cm}^{-1}$  with a resolution of 1  $\text{cm}^{-1}$  with 70 scans in each spectrum. The background spectra of buffer solution were obtained in the same way and were automatically subtracted by the software (Opus 7.0 Bruker).

The ATR-FTIR microscopy measurements were performed with the Simex Mikran-3 microscope according to the previously published methodics.<sup>20</sup> The ATR-FTIR spectra were recorded in the region of 3000–900  $\text{cm}^{-1}$  with 2  $\text{cm}^{-1}$  spectral resolution. For each spectrum, 70 scans were averaged. The background was taken according to the measurement position. The spectra and images were analyzed using the Puma software.

**2.2.2. DSC.** Thermal analysis was conducted through a differential scanning calorimeter (DSC, DSC204F1) (NETZSCH-Germany). A precise amount of samples was loaded into an aluminum pan and thermally scanned from 25 °C to 320 °C at 10 °C  $\text{min}^{-1}$  in N<sub>2</sub> atmosphere.

**2.2.3. PXRD.** The PXRD patterns were registered by a Rigaku SmartLab (Tokio, Japan) equipped with a copper X-ray anode tube. The settings for X-ray generation were 60 kV and 1.5 kW. The scanning range was 1.5–80.0° in increments of 5° per second.



**2.2.4. ROESY.** NMR spectra of the [Rut $\subset$  $\beta$ -CD] complex were measured at 278 K in D<sub>2</sub>O with a Bruker AVANCE 600 MHz spectrometer equipped with a triple resonance (<sup>1</sup>H, <sup>13</sup>C and <sup>15</sup>N) pulsed field *z* gradient probe. 1D NMR spectra were processed and analyzed using the Mnova software (Mestrelab Research, Spain). 2D NMR ROESY (300 ms spin lock time) and DQF-COSY spectra were processed by NMRPipe<sup>21</sup> and analyzed using NMRFAM-SPARKY.<sup>22</sup>

### 2.3. Determining the binding center using theoretical calculations

The GFN2-xTB method, with parameters optimized for 86 elements in the periodic table, is applicable to the examination of different systems, including organic compounds.<sup>23</sup> The energy calculated by the GFN2-xTB method includes van der Waals interactions, hydrogen interactions, and halogen interactions; which are crucial to the study of interactions between organic molecules. The detailed information about the calculation method, including the influence of the solvents, was conducted in the same manner as in our previous work.<sup>19,23</sup>

The possible interaction configurations between Rut and  $\beta$ -CD are similar to those between Rut and hydroxypropyl cyclodextrin:<sup>19</sup> the Rut molecule can direct its A or B end into the  $\beta$ -CD cavity through mode I or mode II (Fig. 1). There are a total of four possible configurations denoted IA, IB, IIA, and IIB.

The interaction energy ( $E_{\text{int}}$ ) between Rut and  $\beta$ -CD is computed as follows:

$$E_{\text{int}} = E(\text{complex}) - E(\text{Rut}) - E(\beta\text{-CD}) \quad (1)$$

where  $E(\text{complex})$ ,  $E(\text{Rut})$ , and  $E(\beta\text{-CD})$  are the energies of the inclusion complex [Rut $\subset$  $\beta$ -CD], Rut, and  $\beta$ -CD, respectively.

### 2.4. Antioxidant activity

**2.4.1. Antioxidant activity measurements.** The DPPH radical method was employed to evaluate antioxidant activity. Briefly, 5 mL of DPPH (concentration  $3.8 \times 10^{-5}$  M, in ethanol)

was added into test tubes containing partial volumes of rutin solutions or complexes of varying concentrations (in the range  $4 \times 10^{-6}$  M  $\div 8.3 \times 10^{-5}$  M), followed by the addition of ethanol. The total volume was 10 mL. The tubes were shaken well and incubated for 30 minutes in the dark. Then, the OD values at 517 nm were determined using the UV-vis spectrophotometer. The percentage of DPPH free radical scavenging activity ( $P$ ) was determined according to the following formula:

$$P = \frac{OD_s - OD_i}{OD_s} \times 100\% \quad (2)$$

where  $OD_s$  and  $OD_i$  are the optical density value of the test samples, containing rutin or complex and optical density value of a test sample, containing 5 mL of DPPH solution and 5 mL of ethanol, respectively.

Based on the percentage of DPPH free radical scavenging activity, the linear correlation equation between the concentration of drug (rutin or complex) and the percentage of DPPH free radical scavenging was determined. Antioxidant activity was defined as the amount of antioxidant necessary to decrease the initial DPPH concentration by 50% (EC<sub>50</sub>). The lower the EC<sub>50</sub> value, the higher the antioxidant activity.

**2.4.2. Determination of antioxidant mechanism by theoretical calculations.** The antioxidant activity of rutin before and after complexation with  $\beta$ -cyclodextrin was examined and elucidated through theoretical calculations. Due to the presence of phenolic-OH groups, the antioxidant activity of rutin can be explained by the antioxidant mechanism of phenolic compounds.

The antioxidant reactions of phenolic compounds are commonly examined through three primary mechanisms: (i) hydrogen atom transfer (HAT); (ii) two-step reaction: single-electron transfer followed by proton transfer (SET-PT); and (iii) two-step reaction: sequential proton loss electron transfer (SPLET).<sup>24</sup> According to Maryam Farrokhnia<sup>24</sup> the presence of solvents may influence the antioxidant mechanism of phenolic compounds. For instance, in polar solvents such as water and ethanol, the antioxidant mechanism of sargahydroquinoic acid and sargachromanol

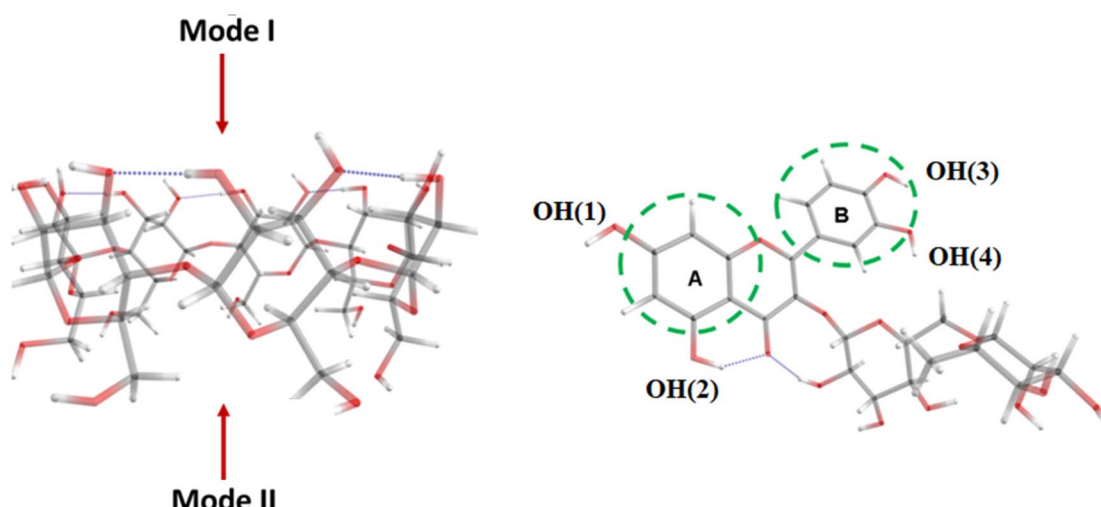


Fig. 1 Interaction modes between rutin and  $\beta$ -CD. Color codes: grey – C, red – O, white – H, and numbering scheme of phenolic –OH groups in Rut molecule.



mainly occurs by the SPLET mechanism. Meanwhile, in non-polar solvents such as benzene, the HAT mechanism predominates.

The parameters characterizing the antioxidant ability corresponding to the HAT, SET, and SPLET mechanisms such as bond-dissociation energy (BDE), ionization potential (IP), PDE (proton dissociation enthalpy), proton affinities (PA), and electron transfer enthalpy (ETE) were calculated according to the enthalpies ( $H$ ) of the species as follows:

$$\text{BDE} = H(\text{Rut-O}^\bullet) + H(\text{H}^\bullet) - H(\text{Rut-OH}) \quad (3a)$$

$$\text{IP} = H(\text{Rut-OH}^{\bullet+}) + H(\text{e}^-) - H(\text{Rut-OH}) \quad (3b)$$

$$\text{PDE} = H(\text{Rut-O}^\bullet) + H(\text{H}^+) - H(\text{Rut-OH}^{\bullet+}) \quad (3c)$$

$$\text{PA} = H(\text{Rut-O}^-) + H(\text{H}^+) - H(\text{Rut-OH}) \quad (3d)$$

$$\text{ETE} = H(\text{Rut-O}^\bullet) + H(\text{e}^-) - H(\text{Rut-O}^-) \quad (3e)$$

where the Rut-X (X = H, O, OH) notations represent the Rut molecule with the X functional groups. Enthalpies of proton  $\text{H}^+$  and electron  $\text{e}^-$  were assumed as 6.1398 and 3.351  $\text{kJ mol}^{-1}$ , respectively.<sup>25,26</sup>

Since the Rut molecule possesses four phenolic OH groups (Fig. 1), the BDE values will be determined for each of the four OH groups in both the Rut molecule and the  $[\text{Rut} \subset \beta\text{-CD}]$  complex. The BDE parameter (eqn (6a)) can be used to disclose the ability of the OH groups to undergo homogeneous dissociation and produce free radicals; the lower the BDE value, the higher the antioxidant activity. The SET-PT mechanism is described by IP and PDE values from  $\text{Rut-OH}^{\bullet+}$ . Compounds with lower IP and PDE values are considered as more effective antioxidants. Finally, in the SPLET mechanism, the first step reaction enthalpy (PA) and the reaction enthalpy of electron abstraction (ETE) are two crucial parameters for determining radical scavenging activity.

For clarification, the characteristic electronic properties such as vertical ionization potential (IP<sub>v</sub>), vertical electron affinity (EA<sub>v</sub>), and global electrophilicity index (GEI) were also evaluated to analyze the influence of the solvents on the antioxidant properties of Rut and  $[\text{Rut} \subset \beta\text{-CD}]$ . The vertical ionization potential/electron affinity was obtained as the energy difference between the ground-state molecule and its ionized species in the same geometry. The GEI, characterized by the electrophilicity or Lewis acidity of various compounds, was derived as follows:

$$\text{GEI} = (\text{IP}_v + \text{EA}_v)^2 / 8(\text{IP}_v - \text{EA}_v) \quad (4)$$

## 3 Results and discussion

### 3.1. Characterization of complex of rutin with $\beta$ -cyclodextrin

**3.1.1. FTIR analysis results.** The results of infrared spectral analysis of the  $[\text{Rut} \subset \beta\text{-CD}]$  complex when compared with samples of Rut and  $\beta\text{-CD}$  are shown in Fig. 2. A broad peak centering at  $3419 \text{ cm}^{-1}$  could be attributed to the valence vibration of the O-H bond.<sup>11</sup> The peak positioning at  $1655 \text{ cm}^{-1}$  could be assigned to the stretching vibration of  $\text{C}=\text{O}$ .<sup>27</sup> The

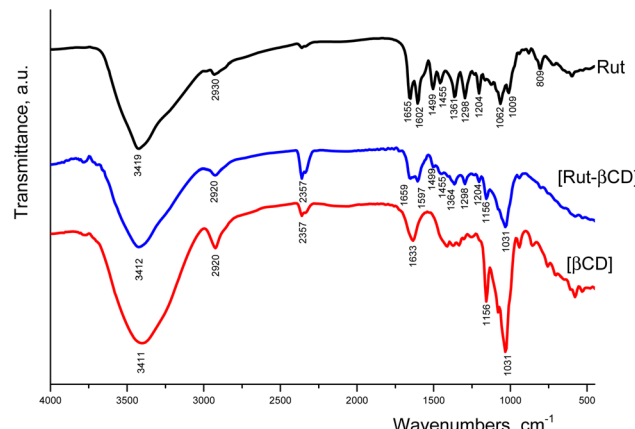


Fig. 2 Fourier infrared spectra of Rut,  $\beta\text{-CD}$  and  $[\text{Rut} \subset \beta\text{-CD}]$  complex.

strong peaks are located at  $1602$  and  $1499 \text{ cm}^{-1}$  corresponding to the valence  $\text{C}=\text{C}$  bond oscillation. This band is considered as pulsating vibrations of the carbon skeleton according to the work.<sup>28</sup> The peaks at  $1361$  and  $1298 \text{ cm}^{-1}$  could be assigned to the  $\text{C}-\text{O}$  bond.<sup>29</sup> Finally characteristic peaks centering at  $1204$ ,  $1062$ , and  $1009 \text{ cm}^{-1}$  represented for the  $\text{C}-\text{O}-\text{C}$  binding within rutin structure.<sup>10,15</sup>

In the infrared spectrum of  $\beta\text{-CD}$ , a strong and broad fringe appeared at  $3411 \text{ cm}^{-1}$ , corresponding to the valence vibration of the  $\text{O}-\text{H}$  bond.<sup>30</sup> The peak centering at  $2920 \text{ cm}^{-1}$  attributed to the valence vibration of the  $\text{C}-\text{H}$  bond in the  $\text{CH}_-$  and  $\text{CH}_2-$  groups of the host molecule.<sup>15</sup> The asymmetric stretching vibration of the  $\text{O}-\text{H}$  bond in the  $\text{C}-\text{O}-\text{H}$  group and  $\text{C}-\text{H}$  bond could be observed at  $1633 \text{ cm}^{-1}$  and  $1156 \text{ cm}^{-1}$ , respectively.<sup>29</sup> The peak at  $1031 \text{ cm}^{-1}$  could be attributed to the valence vibration of the  $\text{C}-\text{O}$  bond in  $\beta\text{-CD}$  at ref. 30

The infrared spectrum of the complex showed the structures of both Rut and  $\beta\text{-CD}$  components. The valence band of the  $\text{O}-\text{H}$  bond in the complex ( $3412 \text{ cm}^{-1}$ ) was narrower and broader than those of  $\beta\text{-CD}$  and pure rutin, suggesting complex formation.<sup>10,15,19</sup> The peak at  $2920 \text{ cm}^{-1}$  could be assigned to the  $\text{C}-\text{H}$  bond. The either largest disappearance of peaks corresponding to the valence vibrations of the  $\text{C}-\text{O}-\text{C}$  bonds (*i.e.*,  $1062$ ,  $1009 \text{ cm}^{-1}$ ) or the decreasing in intensity at the peak centering  $1204 \text{ cm}^{-1}$  inevitably demonstrated that the  $\text{C}-\text{O}-\text{C}$  bond was involved in complex formation.

Since the complex  $[\text{Rut} \subset \beta\text{-CD}]$  is considered as potential biopharmaceutics, we have analyzed the state of the complex components in solutions using ATR-FTIR spectroscopy (Fig. 3). For this purpose, spectra were recorded for saturated solutions of rutin and the complex, as well as a for 50 mM solution of  $\beta\text{-CD}$ .

Firstly, comparing the spectra from powders and solutions, we note the presence of common absorption bands, such as the bands corresponding to the valence  $\text{C}=\text{C}$  bond oscillation in the spectrum of rutin. Main bands positions are presented in Table 1.

It is known that when large molecules are included in cyclodextrins, the interaction will be most pronounced with one



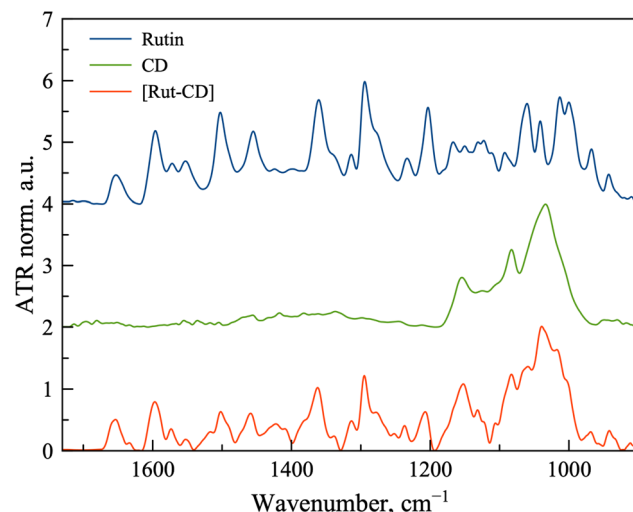


Fig. 3 ATR-FTIR spectra of saturated solutions of Rutin (blue line) and [Rutin- $\beta$ -CD] complex (red line), 50 mM solution of  $\beta$ -CD (green line). 0.02 M sodium – phosphate buffer solution, pH 7.4., 22 °C. Spectra are min–max normalized for better representation.

Table 1 Main band positions in the ATR-FTIR spectra of saturated solutions of Rutin and [Rutin- $\beta$ -CD] complex. 0.02 M sodium-phosphate buffer solution, pH 7.4, 22 °C

Band position, $\text{cm}^{-1}$ /band assignment	Rut	[Rutin- $\beta$ -CD]
C–O–C	1203	1207
C=C	1503	1502, 1491 shoulder
C=C	1596	1597
C=O	1653	1654

of the fragments of the guest molecule. In the case of rutin, there are two key moieties to be considered – carbohydrate and aromatic. A comparison of the spectra of rutin and the complex

in the absorption region of the C–O–C valence bond, characteristic of the carbohydrate part, shows a shift of the characteristic band from 1203 to 1207  $\text{cm}^{-1}$ , which indicates interaction with the oligosaccharide backbone of cyclodextrin.

In this case, the absorption band of the C=C aromatic ring at 1596  $\text{cm}^{-1}$  and the absorption band of the C=O bond at 1653  $\text{cm}^{-1}$ , located on the ring, shift only slightly. A more interesting finding is the formation of a shoulder at 1491  $\text{cm}^{-1}$  in the absorption band of 1503  $\text{cm}^{-1}$ . This band also refers to the stretching vibrations of the C=C bond in the aromatic ring. The formation of a shoulder indicates a change in the micro-environment of the aromatic ring, apparently due to complex formation.

Thus, it is likely that rutin is indeed included in the cyclodextrin torus, and the complexation can additionally be stabilized by the binding of carbohydrate fragments of the guest and the host.

To obtain more detailed information on the distribution of Rutin and  $\beta$ -CD we have studied the powder samples of [Rutin- $\beta$ -CD] with ATR-FTIR microscopy. Microscopic examination of the complex reveals morphologically homogeneous elements (Fig. 4). Thus, we have conducted mapping in the selected area. In each point the ATR-FTIR spectrum was registered. To control the rutin content, the 1360  $\text{cm}^{-1}$  band corresponding to C–O oscillations was used (Fig. 4 upper line). To control the cyclodextrin content, the 1080  $\text{cm}^{-1}$  band corresponding to C–O–C oscillations was used (Fig. 4 down line). Comparison of mappings across these bands shows that cyclodextrin and rutin are distributed evenly throughout the sample, confirming complex formation.

**3.1.2. DSC analysis results.** Differential scanning calorimetry (DSC) measurements of rutin,  $\beta$ -cyclodextrin and complex were conducted to reveal the differences in the composition of “guest” molecules before and after complexation, as shown in Fig. 5. The results demonstrated that the rutin sample exhibited

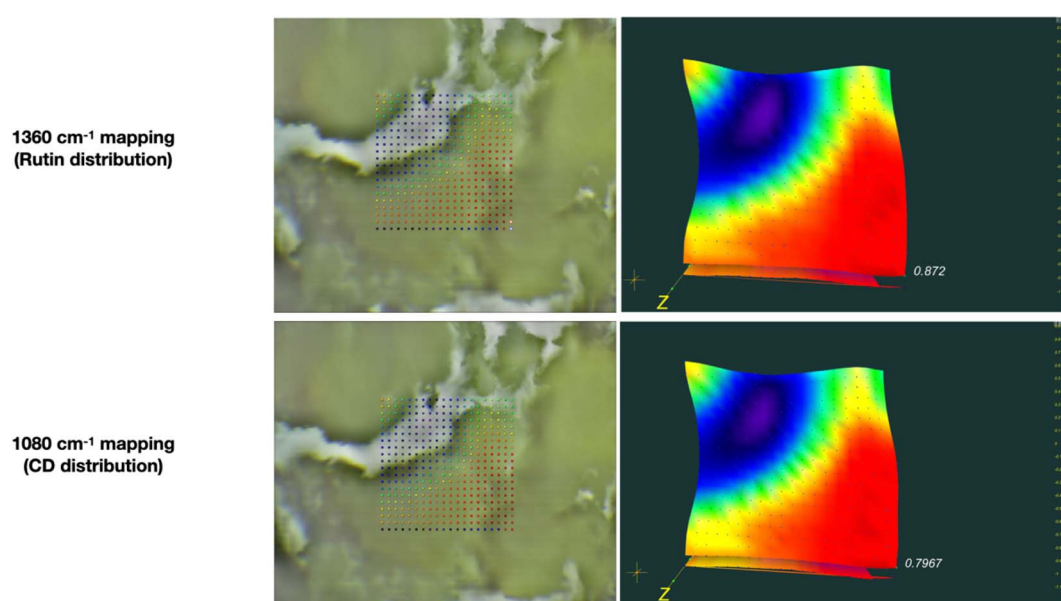


Fig. 4 ATR-FTIR mapping for [Rutin- $\beta$ -CD] complex powder. Mapping area is 302  $\times$  302 microns. 15 $\times$  ATR objective.



a broad endothermic peak at 160 °C, corresponding to the melting point of rutin. The DSC curve of  $\beta$ -CD indicates the release of water molecules from the inner cavity of  $\beta$ -CD, which coincides to a peak at 123 °C (the melting point).

The heat profiles of the complex [Rut $\subset$  $\beta$ -CD] and Rut and  $\beta$ -CD suggested that the endothermic peak of  $\beta$ -CD in the complex is 104 °C, which was a small difference, but the peak intensity was significantly lower than those with  $\beta$ -CD. Especially, the endothermic peak of rutin in the complex was significantly low and nearly disappeared. This piece of evidence indicated rutin- $\beta$ -CD interaction and a portion of the rutin molecule had entered into the hollow cavity of  $\beta$ -CD and obtained a complex.

**3.1.3. PXRD analysis.** In order to discover more details in the interaction between Rut and CD in a solid state, we have obtained powder X-ray diffraction (PXRD) patterns (Fig. 6). The PXRD pattern of Rut (blue line) has narrow peaks, indicating the crystalline nature. The PXRD pattern of the [Rut $\subset$  $\beta$ -CD] complex (red line) is different from patterns of Rut. One could

observe a significant decrease of the intensity of Rut signals, but the main pattern remained the same. The difference between these patterns confirms the formation of the guest–host complex formation.

**3.1.4. ROESY analysis.** 2D ROESY NMR (Rotating frame nuclear Overhauser Effect Spectroscopy) spectroscopy is a powerful method to study inclusion complexes of cyclodextrins as big enough ( $M_w > 1000$ ) molecules. Fig. 7 demonstrates the major region of the 2D ROESY NMR spectra for the Rut protons and the glucose protons of  $\beta$ -CD. Obtained data are in a good agreement with previously published data as concerning chemical shifts as concerning nuclear Overhauser effect.<sup>16</sup> These results also confirm complex formation.

### 3.2. Antioxidant activity

The ability to scavenge DPPH free radicals of rutin and complex is shown in Fig. 8. The antioxidant activity of both rutin and complex increased with the increasing of sample concentration (ranging from  $4.7 \times 10^{-7}$  mol L<sup>-1</sup> to  $2.6 \times 10^{-5}$  mol L<sup>-1</sup>) after 30 minutes of experiments.

The regression equations show a well-correlation between the percentage of DPPH radical scavenging activity and the drug concentrations. The obtained EC<sub>50</sub> values are represented in Table 2.

The data showed that complex formation slightly increased the antioxidant activity of rutin corresponding to the decrease of EC<sub>50</sub> values from  $1.547 \times 10^{-5}$  mol L<sup>-1</sup> to  $1.227 \times 10^{-5}$  mol L<sup>-1</sup>, which agreed with some previous studies.<sup>10,16</sup> Calabro M. L. evaluated the antioxidant activity of the rutin and its complex against lipid peroxidation induced by FeSO<sub>4</sub>.<sup>10</sup> The results showed that, complex formation with  $\beta$ -CD improved the antioxidant activity of rutin, as a result of the increased solubility in the biological moiety.<sup>10</sup> Besides that, the antioxidant capacity of phenolic compound is thought to be closely associated with its hydrogen-donating ability,<sup>16</sup> the increase in the antioxidant activity of rutin after complex formation with  $\beta$ -CD was probably to be changed in its hydrogen-donating capacity, as a result of the complexation. The hydrogen bonds were formed between hydrogen atoms in the hydroxyl groups of rutin with the oxygen atoms of  $\beta$ -CD. These bonds would weaken the covalent bonds between hydrogen and oxygen in the hydroxyl groups, which in turn would make the hydrogen donation by the hydroxyl groups of rutin becoming easier. To confirm this, in the next part the interaction in the complex and antioxidant mechanism have been investigated.

### 3.3. Interactions between rutin and $\beta$ -CD and the effect of solvents on the inclusion complexation

The calculated interaction energies (in kcal mol<sup>-1</sup>) between rutin and  $\beta$ -CD in the vacuum and in different solvents are presented in Table 3.

The calculation results indicate that the energy differences between configurations fluctuate within a few kcal mol<sup>-1</sup>, with the IA and IIB configurations differing by approximately 2–3 kcal mol<sup>-1</sup>. It is indeed possible for multiple configurations to coexist. However, the configuration of the inclusion complex

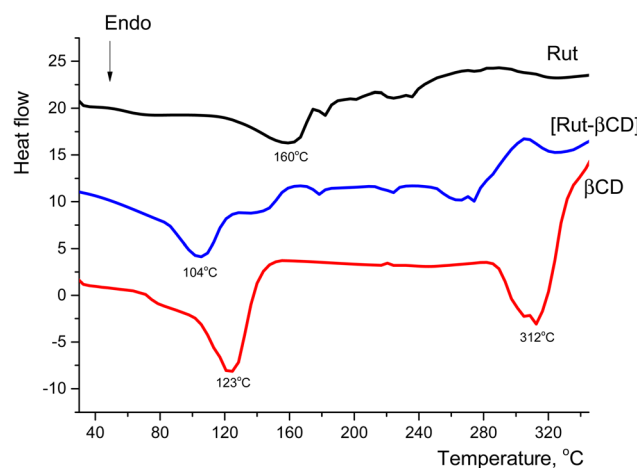


Fig. 5 DSC curves of rutin,  $\beta$ -CD and complex.

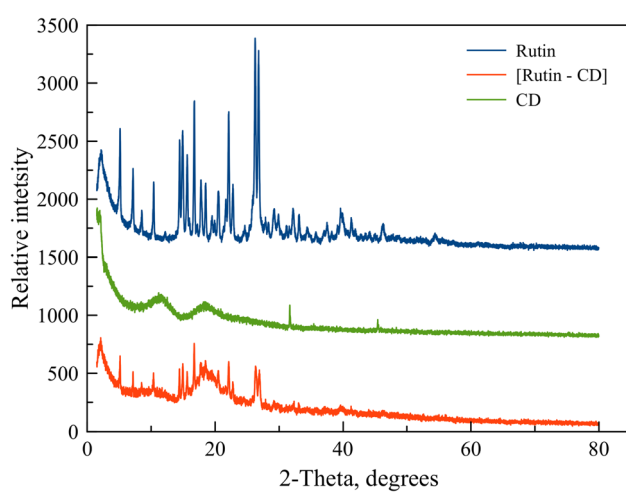


Fig. 6 PXRD patterns for Rut (blue), CD (green) and [Rut $\subset$  $\beta$ -CD] complex (red).



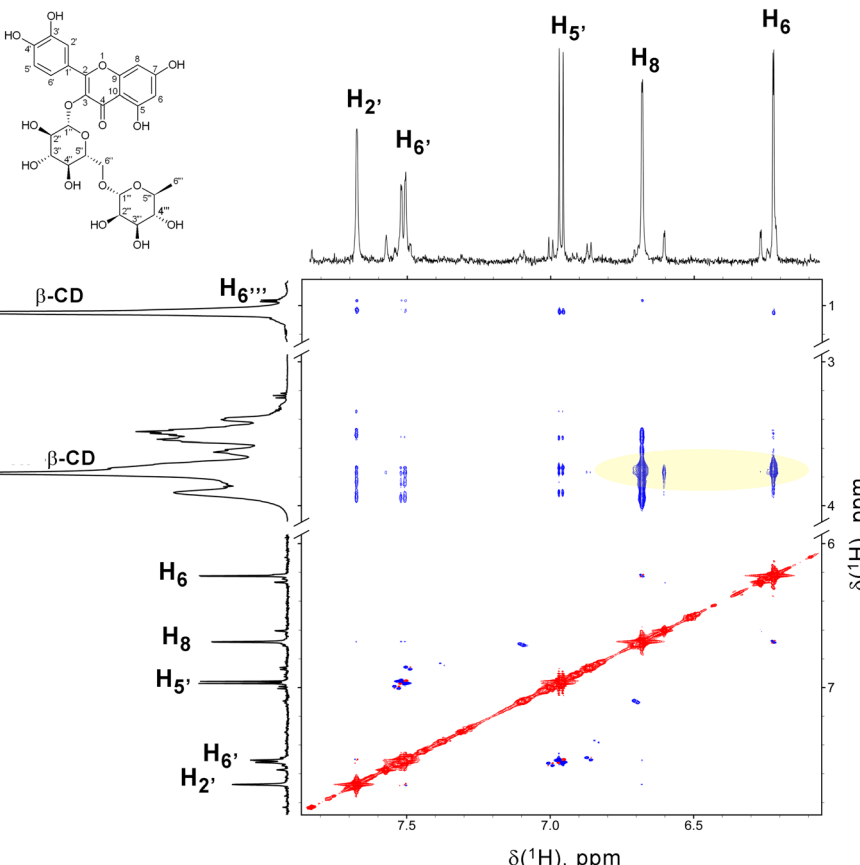


Fig. 7 Fragment of the 2D ROESY spectrum of a solution of the rutin complex with  $\beta$ -CD in  $\text{D}_2\text{O}$ , measured at 278 K and 600 MHz  $^1\text{H}$  resonance frequency. Signals with positive and negative intensity are shown in red and blue, respectively. The yellow oval highlights the cross peaks between the protons H6 and H8 of rutin and the protons of glucose residues  $\beta$ -CD, indicating their spatial proximity.

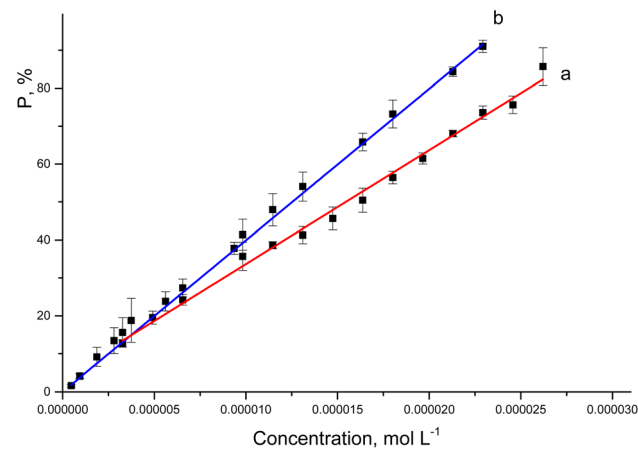


Fig. 8 The correlation equations between the percentage of DPPH radical scavenging activity of rutin (a) or  $[\text{Rut} \subset \beta\text{-CD}]$  (b) and their concentrations.

with the lowest energy is the most favored, exhibiting the highest probability of occurrence. In a vacuum, rutin preferentially interacts with  $\beta$ -CD, forming the IIB complex. This motif is associated with the insertion of rutin into the small-sized empty cavity of the macrocycle. The IA configuration, with an energy only 1.9 kcal mol<sup>-1</sup> higher than the IIB

configuration, also suggests the feasible existence of an inclusion complex in this structural form. This scenario was also observed in the case of ethanol and DMSO solvents. Nevertheless, rutin primarily penetrates the small cavity of  $\beta$ -CD *via* the A-terminal, creating the complex IIA preferable to IIB in water. The interaction between  $\beta$ -CD and Rut through the I direction, *i.e.*, from the large cavity side of  $\beta$ -CD, is likewise thermodynamically favorable due to the negative values of  $E_{\text{int}}$ . However, mode I is less preferred than mode II from the energy-point-of-view, which can be explained as: the Rut- $\beta$ -CD atoms distance is closer, which results in greater interaction particularly the vDW interaction in mode II. It is noteworthy that the Rut- $\beta$ -CD interaction configurations are considerably different from those investigated between Rut and hydroxypropyl- $\beta$ -CD (HP- $\beta$ -CD) interaction.<sup>19</sup> This could be explained by the structural difference between  $\beta$ -CD and HP- $\beta$ -CD. Since the  $\beta$ -CD lacks the bulky substituents (hydroxypropyl) seen in the HP- $\beta$ -CD, the Rut molecule may readily enter the cavity through mode II.

It possibly demonstrates that the interaction energy is slightly negative in ethanol or DMSO. Thus, the principal interaction forces can be attributed to non-covalent forces (*e.g.*, the vDW interaction and hydrogen bonding). To identify the locations of weak interactions and intuitively capture their nature, we analyze the dependence of the reduced density



Table 2 The percentage of DPPH radical scavenging activity of rutin or [Rut $\subset$  $\beta$ CD] (y) and concentrations of drug (x)

Items	Correlation equation	Regression coefficient	$EC_{50} \times 10^5$ , mol L $^{-1}$
Rut	$y = 3.56979 + 3.0014 \times 10^6 x$	0.993	1.547
[Rut $\subset$ $\beta$ CD]	$y = 1.93228 + 3.9191 \times 10^6 x$	0.996	1.227

Table 3 Calculated interaction energies ( $E_{int}$ , kcal mol $^{-1}$ ) between rutin and  $\beta$ -CD in the vacuum and in the different solvents by GFN2-xTB method

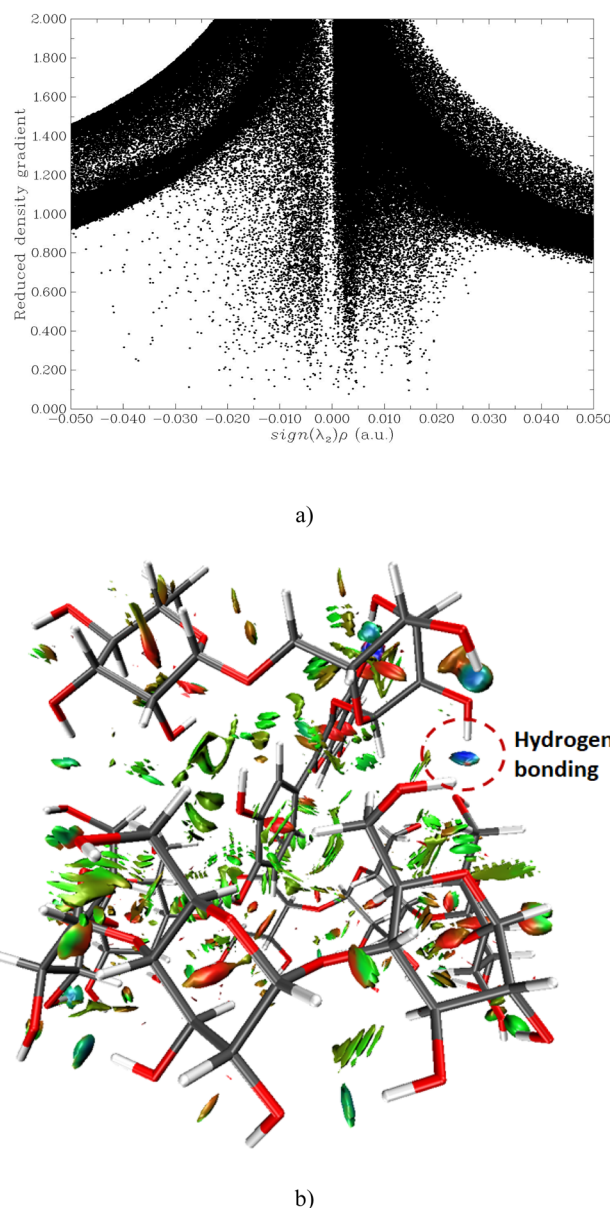
Environment	IA	IB	IIA	IIB
Vacuum	-47.92	-39.52	-39.02	-49.82
Water	-20.44	-11.37	-25.01	-17.78
Ethanol	-17.60	-10.14	-11.16	-19.21
DMSO	-5.23	-5.45	-5.96	-7.24

gradient (RDG) on the product of the sign of  $\lambda_2$  and  $\rho$ .<sup>31</sup> Here,  $\lambda_2$  is the second largest eigenvalue of the Hessian matrix of the electron density, and  $\rho$  represents the electron density of complex IIB in a vacuum.

In Fig. 9(a), two spikes are observed in the range of -0.01 to 0.01 a.u., corresponding to van der Waals interactions (indicated by the green area in Fig. 9(b)). A spike at approximately 0.02 a.u. is indicative of steric effects (denoted by the red area in Fig. 9(b)), while a spike between -0.02 and -0.04 corresponds to hydrogen bonding interactions (represented by the blue area in Fig. 9(b)).

In the presence of solvents, the interaction capability toward  $\beta$ -CD of rutin decreases in the order of water > ethanol > DMSO, correlating to a decrease in the absolute values of  $E_{int}$  in this order. However, the interaction between rutin and  $\beta$ -CD is not substantially different in ethanol or DMSO.

The frontier molecular orbitals of the studied substances were evaluated to understand the nature of the inclusion complexes' formation. The highest occupied molecular orbital (HOMO) and the lowest unoccupied molecular orbital (LUMO) analysis can provide additional information about the electron transfer (if any) between components in the inclusion complex. The HOMO and LUMO of Rut and  $\beta$ -CD remain as transferring from the vacuum to aqueous solution (Fig. 10 and 11). However, a clear difference in the vacuum and water environments appears in the HOMO and LUMO of the [Rut $\subset$  $\beta$ -CD] encapsulated complex. In the vacuum, the HOMO distribution of [Rut $\subset$  $\beta$ -CD] complex is condensed on the host molecule (*i.e.*,  $\beta$ -CD) while the LUMO is completely concentrated on the guest molecule. As a result, an interaction induces electron transfer within the inclusion complex. However, both the HOMO and LUMO of [Rut $\subset$  $\beta$ -CD] are mainly contributed by rutin in aqueous environment. Thus, the interaction between rutin and  $\beta$ -CD decreases in water in comparison to the vacuum. This is completely consistent with the calculation results of the total Mulliken charge on the rutin molecule in the inclusion complexes. The total charges on the rutin molecule in the vacuum and in water are  $-0.028e$  and  $+0.004e$ , respectively for the [Rut $\subset$  $\beta$ -CD]-IIA complex. Therefore, there is a significant decrease in charge transfer from the "host" molecule to the "guest" molecule.

Fig. 9 Scatter graph of dependence of RDG on sign  $\lambda_2$  ( $\rho$ ) function (a); the RDG isosurface depicted at an isovalue of 0.8 of IIB complex (b).

In the presence of a solvent, the electronic properties of Rut and [Rut $\subset$  $\beta$ -CD] signifies an alternation. Table 4 presents the results of the IP<sub>v</sub>, EA<sub>v</sub>, and GEI parameters calculation of Rut and [Rut $\subset$  $\beta$ -CD] in the vacuum and in various solvents.

The findings prove that the presence of solvents enhances the ionization potential and electron affinity of both Rut and [Rut $\subset$  $\beta$ -CD], and thus, increased the GEI index of the studied



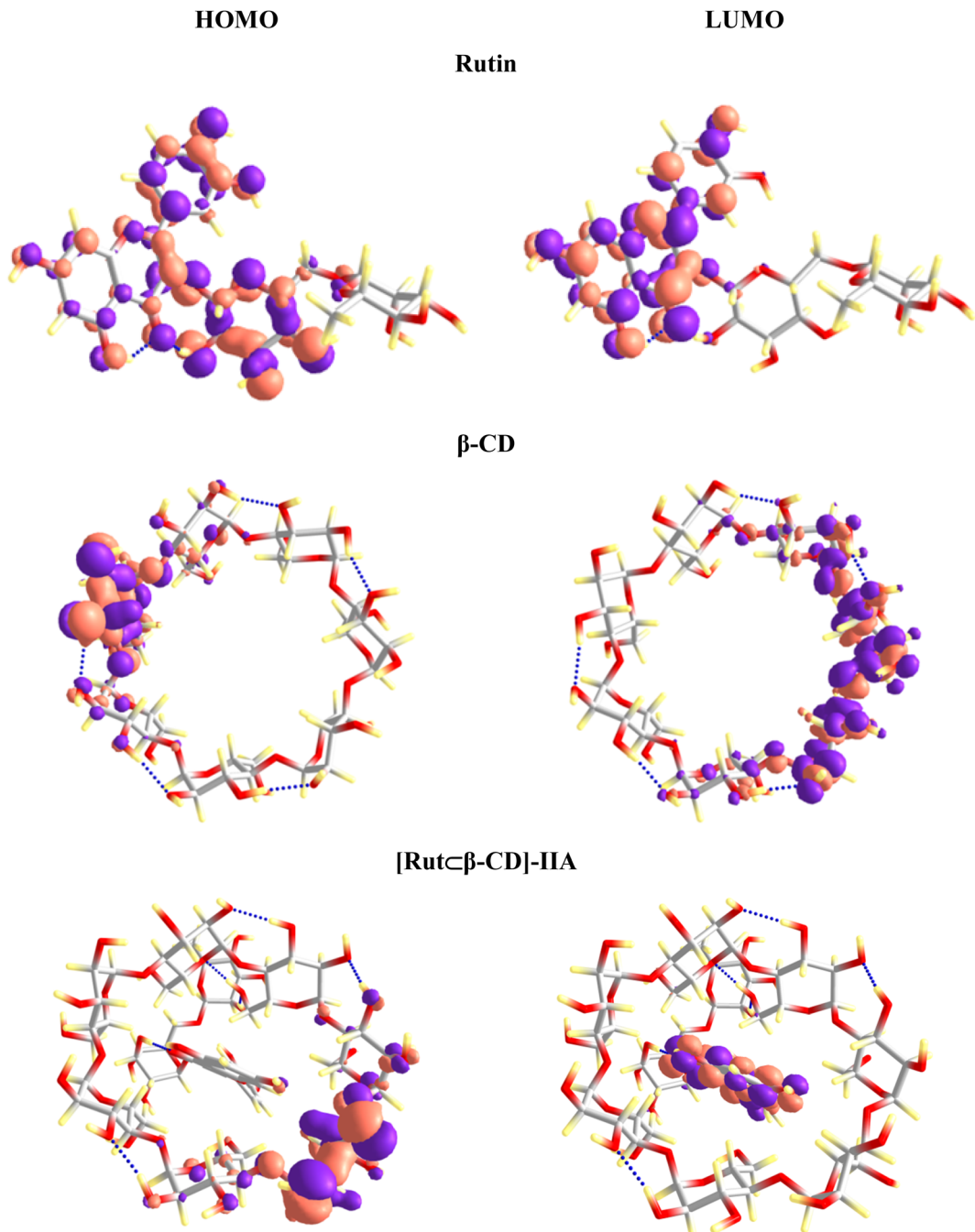


Fig. 10 HOMO and LUMO of the studied systems in the vacuum.

systems. The order of GEI values in Rut and  $[\text{Rut} \subset \beta\text{-CD}]$  is water > ethanol  $\approx$  DMSO > vacuum. In other words, Rut and  $[\text{Rut} \subset \beta\text{-CD}]$  facilitate the charge-transfer process under the existence of water, which can impact the antioxidant capacity of Rut and  $[\text{Rut} \subset \beta\text{-CD}]$  in various solvents.

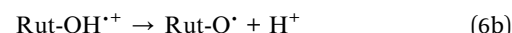
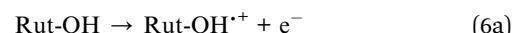
#### 3.4. Antioxidant mechanisms of Rut and $[\text{Rut} \subset \beta\text{-CD}]$

In this study, the antioxidant capacity of Rut and  $[\text{Rut} \subset \beta\text{-CD}]$  in solvents such as water, ethanol, and DMSO was analyzed using three mechanisms: HAT, SET-PT, and SPLET as follows:

- HAT mechanism:



- SET-PT mechanism:



- SPLET mechanism:



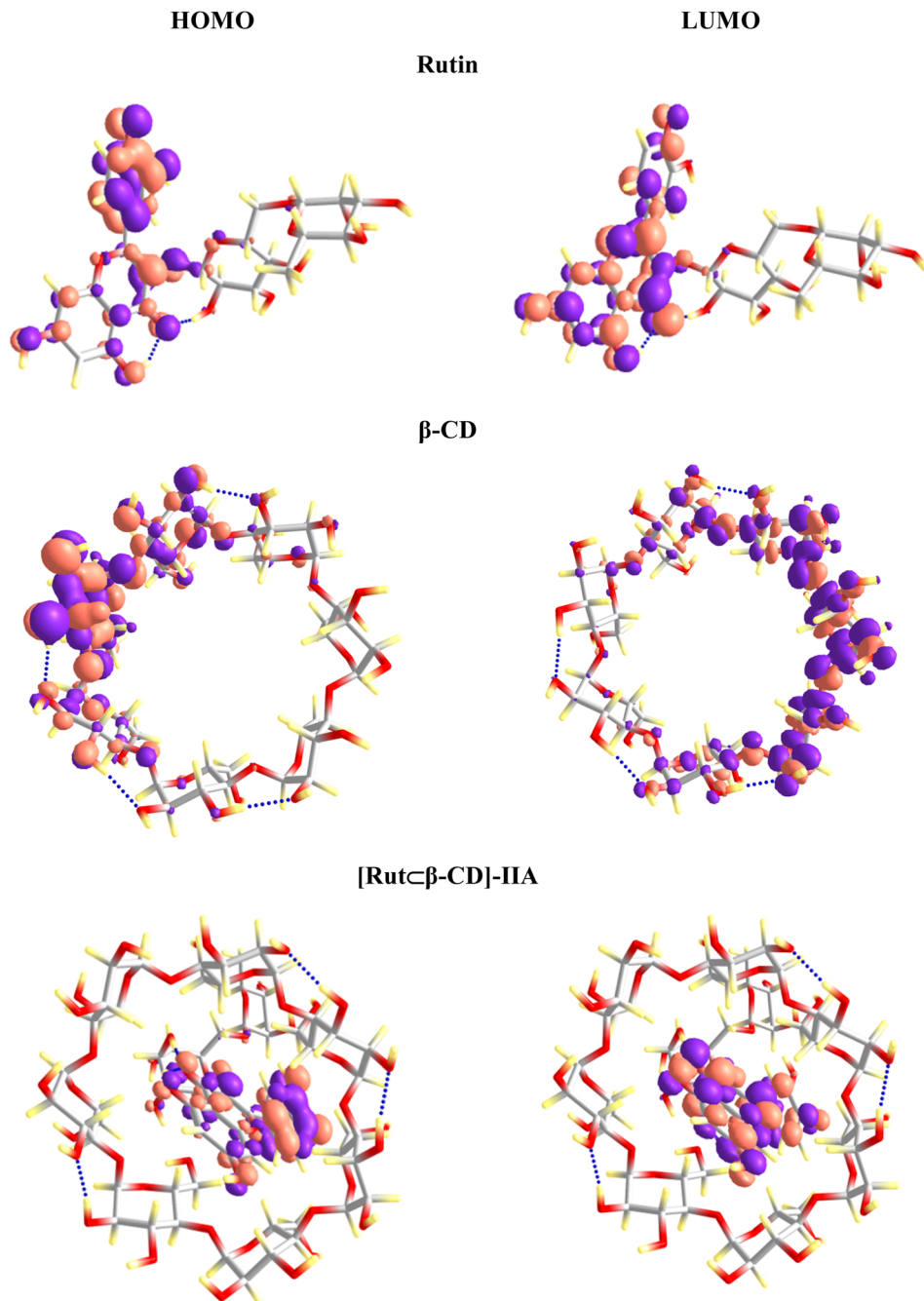
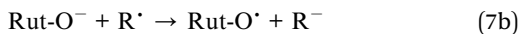


Fig. 11 HOMO and LUMO of the studied systems in water.



Three antioxidant mechanisms of Rut and  $[\text{Rut-}\beta\text{-CD}]$  are considered. Table 5 presents the results of the computation of the characteristic parameters (BDE, IP, PDE, PA and ETE) for the these mechanisms.

The HAT mechanism is characterized by the BDE value of the O-H bonds.

The BDE values of Rut and  $[\text{Rut-}\beta\text{-CD}]$  in various environments change by a slight amount. Most of the BDE values of  $[\text{Rut-}\beta\text{-CD}]$  are lower than those of Rut, except for some values in the-OH groups (2), (3), and (4) in DMSO. A difference between Rut and  $[\text{Rut-}\beta\text{-CD}]$  antioxidant ability maintains according to the HAT mechanism. This is consistent with the structure of the  $[\text{Rut-}\beta\text{-CD}]$  complex in which Rut only partially “burrows” into the hollow cavity of  $\beta\text{-CD}$ , and the active-OH groups of Rut are less affected by interactions with  $\beta\text{-CD}$ , since the interactions are mainly vdW interactions and not chemical interactions.



**Table 4** Electronic properties of Rut and [Rut $\subset$  $\beta$ -CD] in different solvents

	Vacuum	Water	Ethanol	DMSO
<b>Rut</b>				
IP <sub>v</sub> , eV	7.5157	6.3415	6.1482	6.2070
EA <sub>v</sub> , eV	1.4537	2.7724	2.5832	2.6018
GEI, eV	1.6589	2.9090	2.6732	2.6904
<b>[Rut<math>\subset</math><math>\beta</math>-CD]</b>				
IP <sub>v</sub> , eV	7.6291	6.6077	6.2168	6.2353
EA <sub>v</sub> , eV	2.5368	3.5668	2.9528	2.9219
GEI, eV	2.5368	4.2554	3.2200	3.1635

**Table 5** The BDE, IP, PDE, PA and ETE (in kcal mol<sup>-1</sup>) calculated values for Rut and [Rut $\subset$  $\beta$ -CD] in different environments

		Antioxidant				
Environments	site	BDE	IP	PDE	PA	ETE
<b>Rut</b>						
Vacuum	OH(1)	107.74	270.82	83.82	157.33	198.10
	OH(2)	114.33		90.40	170.65	191.37
	OH(3)	103.27		79.34	160.92	190.04
	OH(4)	100.12		76.19	163.52	184.29
Water	OH(1)	109.31	243.15	112.49	121.79	234.65
	OH(2)	110.36		113.54	126.07	231.42
	OH(3)	103.73		106.91	126.23	224.63
	OH(4)	101.92		105.10	120.30	228.75
Ethanol	OH(1)	108.39	244.12	110.45	124.01	231.36
	OH(2)	110.82		112.88	130.12	227.68
	OH(3)	103.14		105.20	128.23	221.89
	OH(4)	100.86		102.92	129.37	218.47
DMSO	OH(1)	110.04	243.59	111.43	128.46	227.36
	OH(2)	112.97		114.37	136.03	222.74
	OH(3)	104.31		105.71	132.57	217.53
	OH(4)	101.96		103.36	133.54	214.21
<b>[Rut<math>\subset</math><math>\beta</math>-CD]</b>						
Vacuum	OH(1)	106.68	261.43	92.13	153.44	200.92
	OH(2)	113.06		98.52	166.98	193.76
	OH(3)	101.48		86.94	150.54	198.64
	OH(4)	97.28		82.74	149.90	195.08
Water	OH(1)	108.47	245.69	109.11	116.81	238.79
	OH(2)	105.21		105.85	115.81	236.53
	OH(3)	105.19		105.83	122.64	229.69
	OH(4)	97.28		97.92	114.56	229.85
Ethanol	OH(1)	105.22	239.63	111.76	123.86	228.33
	OH(2)	110.55		117.09	130.31	227.21
	OH(3)	110.55		117.09	120.84	236.68
	OH(4)	95.34		101.88	119.26	223.05
DMSO	OH(1)	109.93	241.84	113.08	127.82	227.90
	OH(2)	113.00		116.15	135.23	223.56
	OH(3)	113.00		116.15	126.99	231.80
	OH(4)	102.26		105.41	127.34	220.70

Among the four OH sites, the calculated BDE value for the OH(4) group is always the lowest, suggesting that this is the most effective antioxidant activity site in the Rut molecule as well as in the [Rut $\subset$  $\beta$ -CD] complex. Meanwhile, the BDE value for the OH(2) group is the highest in most cases, indicating the least effective of this OH group. This is explained that the OH(2)

group is stabilized through the formation of a hydrogen bond with the adjacent OH group of the tail of the Rut molecule.

The analysis of the solvent impact on the BDE values of Rut and [Rut $\subset$  $\beta$ -CD] revealed that the solvent had slightly effect. It is noted that the BDE value of OH(4) of [Rut $\subset$  $\beta$ -CD] reduces most greatly in ethanol compared to that of Rut. This is also the lowest BDE value observed among the studied systems. Therefore, the antioxidant properties of [Rut $\subset$  $\beta$ -CD] in solutions with high ethanol concentration may be predicted to be higher than that of Rut. Meanwhile, in the DMSO solvent, the BDE values of both Rut and [Rut $\subset$  $\beta$ -CD] are higher than the corresponding BDE values in other solvents, indicating that the presence of DMSO inhibits the antioxidant activity of both Rut and [Rut $\subset$  $\beta$ -CD].

The SET-PT mechanism is a two-stage antioxidant process involving IP and PDE. The first step of molecular ionization corresponding to the high IP is considered the determining step. The IP values of Rut and [Rut $\subset$  $\beta$ -CD] change significantly from the vacuum to the presence of solvent. In particular, with Rut, the presence of a solvent dramatically reduces the IP compared to that in the vacuum. A similar phenomenon can be observed with [Rut $\subset$  $\beta$ -CD]. However, the IP values of Rut in the solvents are similar, whereas, with [Rut $\subset$  $\beta$ -CD], in ethanol, the obtained IP value is the lowest. This may be attributed to the effect of different solvations. With the lowest IP value calculated in ethanol for [Rut $\subset$  $\beta$ -CD], and the PDE value of the OH(4) group not being too large (about 101 kcal mol<sup>-1</sup>), the SET-PT mechanism is predicted to be possible but it will be more difficult than the HAT mechanism since the IP value is much higher than the BDE value.

The SPLET mechanism consists of two stages and is characterized by PA and ETE. The analysis of the PA and ETE values achieved from the Rut and [Rut $\subset$  $\beta$ -CD] shows that the formation of the insertion complex results in a slight decrease in PA and an increasing in PTE values. Therefore, the antioxidant capacity of [Rut $\subset$  $\beta$ -CD] could lightly change compared with the original Rut according to the SPLET mechanism. The SPLET mechanism is predicted to be more probable than the SET-PT mechanism but less likely than the HAT mechanism if PA values centering between 110-120 kcal mol<sup>-1</sup> and ETE values are lower than those of IP values.

Our calculated results align with previous studies on the influence of inclusion complexation on the antioxidant activity of flavonoids. For instance, Zheng *et al.*<sup>32</sup> demonstrated that CD inclusion complexation enhances the antioxidative activity of apigenin in aqueous ethanol solutions. However, while the solvent can alter the antioxidant mechanism of apigenin, the HAT mechanism remains dominant for rutin across all solvents. Several studies have demonstrated that the SPLET mechanism is thermodynamically favored in polar solvents such as water, DMSO, and methanol.<sup>32-34</sup> Our findings also highlight the influence of solvents on the propensity for the SPLET antioxidant mechanism, with PA increasing in the order of water < ethanol < DMSO. It is important to note that the differences between PDA and BDE across these solvents are minimal, indicating that the antioxidant activity of rutin and the [Rut $\subset$  $\beta$ -CD] inclusion complex may occur through multiple mechanisms simultaneously within a given solvent.



## 4 Conclusions

The complex of rutin and  $\beta$ -cyclodextrin was successfully synthesized. The results of FTIR spectroscopy in powders and solutions and DSC analysis exhibited that a portion of the rutin molecule had entered the hollow cavity of  $\beta$ -CD and formed a complex. According to the ATR-FTIR microscopy of complex powder both Rut and  $\beta$ -CD are distributed eventually confirming complex formation. The favorable interaction configurations between Rut and  $\beta$ -CD were considerably different from the previously reported interaction between Rut and hydroxypropyl- $\beta$ -CD (HP $\subset$  $\beta$ -CD). The Rut molecule might enter the cavity of  $\beta$ -CD through mode II. Experimental results showed that the antioxidant activity of rutin increased slightly after complexing with  $\beta$ -CD. The EC<sub>50</sub> concentration at which rutin could neutralize 50% of the free radicals of DPPH in solution after complexation reduced about 20%. The theoretical calculation results were in consistent with the experimental results: there was a slight decrease in the calculated values of BDE, IP, PDE, PA and ETE of rutin in complexation compared with pure rutin. In particular, the calculation results according to the HAT mechanism indicated that among the OH phenolic functional groups, the OH(4) group was the most effective antioxidant activity center of the rutin molecule, while the OH(2) functional group was significantly less effective. Theoretical calculation results also proved that the nature of the solvent (gas or liquid phase, aqueous or mixed solvent, polar or non-polar solvent) had almost no effect on the antioxidant of rutin and complexes.

## Data availability

The authors confirm that the data supporting the findings of this study are available within the article.

## Author contributions

Thi Lan Pham: investigation, formal analysis, data curation, writing – original draft, reviewing and editing. Thi Thu Ha Nguyen: investigation, formal analysis, data curation, writing – original draft. Tuan Anh Nguyen: investigation, formal analysis, data curation. Irina Le-Deygen: investigation, formal analysis, writing – original draft. Thi My Hanh Le: investigation, data curation. Xuan Minh Vu: investigation, formal analysis. Hai Khoa Le: investigation, formal analysis. Van Cuong Bui: formal analysis, data curation. T. R. Usacheva: data curation. Thanh Tung Mai: formal analysis, data curation. Dai Lam Tran: conceptualization, data curation, writing – original draft and reviewing and editing, supervision.

## Conflicts of interest

The authors declare that they have no known competing financial interests or personal relationships that could have appeared to influence the work reported in this paper.

## Acknowledgements

This work was funded by The Vietnam Academy of Science and Technology (VAST) under the grant number NCXS 01.01/22-24. ATR-FTIR microscopy and ATR-FTIR spectroscopy (for solutions) were conducted in Lomonosov Moscow State University with equipment of Developmental program of MSU. The authors are grateful to Lomonosov Moscow State University for the opportunity to use NMR facilities, Svetlana Savelyeva for qualified technical assistance in measuring NMR spectra, and Dr Vladimir Polshakov for assistance in interpreting the NMR spectra. The authors are grateful to Prof. Dr Peter M. Tolstoy, Head of Dep. of Physical Organic Chemistry, Institute of Chemistry, St Petersburg University for help in discussing the results.

## References

- 1 S. A. de Souza Farias, K. S. da Costa and J. B. L. Martins, Comparative analysis of the reactivity of anthocyanidins, leucoanthocyanidins, and flavonols using a quantum chemistry approach, *J. Mol. Model.*, 2023, **29**, 93, DOI: [10.1007/s00894-023-05468-w](https://doi.org/10.1007/s00894-023-05468-w).
- 2 E. Sofic, A. Copra-Janicijevic, M. Salihovic, I. Tahirovic and G. Kroyer, Screening of medicinal plant extracts for quercetin-3rutinoside (rutin) in Bosnia and Herzegovina, *Med. Plants – Int. J. Phytomed. Relat.*, 2010, **2**(2), 97–102, DOI: [10.5958/j.0975-4261.2.2.015](https://doi.org/10.5958/j.0975-4261.2.2.015).
- 3 N. T. Le, T. P. D. Nguyen, D. V. Ho, H. T. Phung and H. T. Nguyen, Green solvents-based rutin extraction from Sophora japonica L, *J. Appl. Res. Med. Aromat. Plants*, 2023, **36**, 100508, DOI: [10.1016/j.jarmap.2023.100508](https://doi.org/10.1016/j.jarmap.2023.100508).
- 4 N. A. Al-Dhabi, M. V. Arasu, C. H. Park and S. U. Park, An up-to-date review of rutin and its biological and pharmacological activities, *EXCLI J.*, 2015, **14**, 59–63, DOI: [10.17179/excli2014-663](https://doi.org/10.17179/excli2014-663).
- 5 A. Taraba and K. Szymczyk, Spectroscopic studies of the quercetin/rutin-nonionic surfactant interactions, *J. Mol. Liq.*, 2022, **360**, 119483, DOI: [10.1016/j.molliq.2022.119483](https://doi.org/10.1016/j.molliq.2022.119483).
- 6 M. Bello, A. Martínez-Muñoz and I. Balbuena-Rebolledo, Identification of saquinavir as a potent inhibitor of dimeric SARS-CoV2 main protease through MM/GBSA, *J. Mol. Model.*, 2020, **26**, 340, DOI: [10.1007/s00894-020-04600-4](https://doi.org/10.1007/s00894-020-04600-4).
- 7 J. Tao, Q. Hu, J. Yang, *et al*, In vitro anti-HIV and-HSV activity and safety of sodium rutin sulfate as a microbicide candidate, *Antiviral Res.*, 2007, **75**(3), 227–233, DOI: [10.1016/j.antiviral.2007.03.008](https://doi.org/10.1016/j.antiviral.2007.03.008).
- 8 P. K. Agrawal, C. Agrawal and G. Blunden, Rutin: A Potential Antiviral for Repurposing as a SARS-CoV-2 Main Protease ( $M^{Pro}$ ) Inhibitor, *Nat. Prod. Commun.*, 2021, **16**(4), 1–12, DOI: [10.1177/1934578X21991723](https://doi.org/10.1177/1934578X21991723).
- 9 T. V. Ilyich, T. A. Kovalenia, E. A. Lapshina, *et al*, Thermodynamic parameters and mitochondrial effects of supramolecular complexes of quercetin with  $\beta$ -cyclodextrins, *J. Mol. Liq.*, 2021, **325**, 115184, DOI: [10.1016/j.molliq.2020.115184](https://doi.org/10.1016/j.molliq.2020.115184).
- 10 M. L. Calabrò, S. Tommasini, P. Donato, *et al*, The rutin/ $\beta$ -cyclodextrin interactions in fully aqueous solution:

spectroscopic studies and biological assays, *J. Pharm. Biomed. Anal.*, 2005, **36**, 1019–1027, DOI: [10.1016/j.jpba.2004.09.018](https://doi.org/10.1016/j.jpba.2004.09.018).

11 J. Liu, S. Zhang, X. Zhao, *et al*, Molecular simulation and experimental study on the inclusion of rutin with  $\beta$ -cyclodextrin and its derivative, *J. Mol. Struct.*, 2022, **1254**, 132359, DOI: [10.1016/j.molstruc.2022.132359](https://doi.org/10.1016/j.molstruc.2022.132359).

12 T. L. Pham, T. R. Usacheva, I. A. Kuz'mina, T. N. Nguyen, *et al*, Effect of cyclodextrin types and reagents solvation on the stability of complexes between B-cyclodextrins and rutin in water-ethanol solvents, *J. Mol. Liq.*, 2020, **318**, 114308, DOI: [10.1016/j.molliq.2020.114308](https://doi.org/10.1016/j.molliq.2020.114308).

13 M. Liu, L. Dong, A. Chen, *et al*, Inclusion complexes of quercetin with three  $\beta$ -cyclodextrins derivatives at physiological pH: Spectroscopic study and antioxidant activity, *Spectrochim. Acta, Part A*, 2013, **115**, 854–860, DOI: [10.1016/j.saa.2013.07.008](https://doi.org/10.1016/j.saa.2013.07.008).

14 E. Basaran, A. A. Ozturk, B. Senel, *et al*, Quercetin, rutin and quercetin-rutin incorporated hydroxypropyl  $\beta$ -cyclodextrin inclusion complexes, *Eur. J. Pharm. Sci.*, 2022, **172**, 106153, DOI: [10.1016/j.ejps.2022.106153](https://doi.org/10.1016/j.ejps.2022.106153).

15 I. M. Savic, I. M. Savic-Gajic and V. D. Nikolic, Enhanceemet of solubility and photostability of rutin by complexation with  $\beta$ -cyclodextrin and (2-hydroxypropyl)- $\beta$ -cyclodextrin, *J. Inclusion Phenom. Macroyclic Chem.*, 2016, **86**, 33–43, DOI: [10.1007/s10847-016-0638-8](https://doi.org/10.1007/s10847-016-0638-8).

16 T. A. Nguyen, B. Liu, J. Zhao, D. S. Thomas and J. M. Hook, An investigation into the supramolecular structure, solubility, stability and antioxidant activity of rutin/cyclodextrin inclusion complex, *Food Chem.*, 2013, **136**(1), 186–192, DOI: [10.1016/j.foodchem.2012.07.104](https://doi.org/10.1016/j.foodchem.2012.07.104).

17 R. Wang, B. Ding and G. Liang, Interaction poses, intermolecular forces, dynamic preferences between flavonoids and maltosyl- $\beta$ -cyclodextrin, *J. Mol. Liq.*, 2022, **346**, 117068, DOI: [10.1016/j.molliq.2021.117068](https://doi.org/10.1016/j.molliq.2021.117068).

18 W. Cai, Y. Chen, L. Xie, *et al*, Characterization and density functional theory study of the antioxidant activity of quercetin and its sugar-containing analogues, *Eur. Food Res. Technol.*, 2014, **238**, 121–128, DOI: [10.1007/s00217-013-2091-x](https://doi.org/10.1007/s00217-013-2091-x).

19 T. L. Pham, T. R. Usacheva, D. A. Alister, *et al*, Thermodynamic parameters and quantum chemical calculations of complex formation between rutin and 2-hydroxypropyl- $\beta$ -cyclodextrin in water-ethanol solvents, *J. Mol. Liq.*, 2022, **366**, 120324, DOI: [10.1016/j.molliq.2022.120324](https://doi.org/10.1016/j.molliq.2022.120324).

20 A. A. Skuderina, A. S. Tychinina, I. M. Le-Deygen, *et al*, The formation of quasi-regular polymeric network of cross-linked sulfobutyl ether derivative of  $\beta$ -cyclodextrin synthesized with moxifloxacin as a template, *React. Funct. Polym.*, 2021, **159**(5), 104811, DOI: [10.1016/j.reactfunctpolym.2021.104811](https://doi.org/10.1016/j.reactfunctpolym.2021.104811).

21 F. Delaglio, S. Grzesiek, G. W. Vuister, G. Zhu, J. Pfeifer and A. Bax, NMRPipe: a multidimensional spectral processing system based on UNIX pipes, *J. Biomol. NMR*, 1995, **6**, 277–293.

22 W. Lee, M. Tonelli and J. L. Markley, NMRFAM-SPARKY: enhanced software for biomolecular NMR spectroscopy, *Bioinformatics*, 2015, **31**, 1325–1327.

23 C. Bannwarth, S. Ehlert and S. Grimme, GFN2-xTB - An Accurate and Broadly Parametrized Self-Consistent Tight-Binding Quantum Chemical Method with Multipole Electrostatics and Density-Dependent Dispersion Contributions, *J. Chem. Theory Comput.*, 2019, **15**, 1652–1671, DOI: [10.1021/acs.jctc.8b01176](https://doi.org/10.1021/acs.jctc.8b01176).

24 M. Farrokhnia, Density Functional Theory Studies on the Antioxidant Mechanism and Electronic Properties of Some Bioactive Marine Meroterpenoids: Sargahydroquinonic Acid and Sargachromanol, *ACS Omega*, 2020, **5**(32), 20382–20390, DOI: [10.1021/acsomega.0c02354](https://doi.org/10.1021/acsomega.0c02354).

25 J. J. Fifen, Thermodynamics of the electron revisited and generalized, *J. Chem. Theory Comput.*, 2020, **9**, 3165–3169, DOI: [10.1021/ct400212t](https://doi.org/10.1021/ct400212t).

26 J. J. Fifen, Z. Dhaouadi and M. Nsangou, Revision of the thermodynamics of the proton in gas phase, *J. Phys. Chem. A*, 2014, **118**, 11090–11097, DOI: [10.1021/jp508968z](https://doi.org/10.1021/jp508968z).

27 Q. Panhwar and S. Memon, Synthesis, characterisation, and antioxidant study of Cr(III)-rutin complex, *Chem. Pap.*, 2014, **68**(5), 614–623, DOI: [10.2478/s11696-013-0494-6](https://doi.org/10.2478/s11696-013-0494-6).

28 E. Pretsch, P. Buhlmann and M. Badertscher, *Structure Determination of Organic Compounds – Tables of Spectral Data*, 2009, Fourth, Revised and Enlarged Edition, 2009.

29 M. K. Ladan, J. Straus, E. T. Benković and S. Kreft, FT-IR-based method for rutin, quercetin and quercitrin quantification in different buckwheat (*Fagopyrum*) species, *Sci. Rep.*, 2017, **7**, 7226, DOI: [10.1038/s41598-017-07665-z](https://doi.org/10.1038/s41598-017-07665-z).

30 H. Sifaoui, A. Modarressi, P. Magri, A. Stachowicz-Kuśnierz, J. Korchowiec and M. Rogalski, Formation of  $\beta$ -cyclodextrin complexes in an anhydrous environment, *J. Mol. Model.*, 2016, **22**, 207–220, DOI: [10.1007/s00894-016-3061-6](https://doi.org/10.1007/s00894-016-3061-6).

31 E. R. Johnson, S. Keinan, P. Mori-Sánchez, J. Contreras-García, A. J. Cohen and W. Yang, Revealing Noncovalent Interactions, *J. Am. Chem. Soc.*, 2010, **132**(18), 6498–6506, DOI: [10.1021/ja100936w](https://doi.org/10.1021/ja100936w).

32 X. Zheng, Y. Du, Y. Chai and Y. Zheng, A DFT-Based Mechanism Analysis of the Cyclodextrin Inclusion on the Radical Scavenging Activity of Apigenin, *Antioxidants*, 2023, **12**(11), 2018, DOI: [10.3390/antiox12112018](https://doi.org/10.3390/antiox12112018).

33 L. Wang, Q. Yang, Y. Li, S. Wang, F. Yang and X. Zhao, How the functional group substitution and solvent effects affect the antioxidant activity of (+)-catechin?, *J. Mol. Liq.*, 2021, **327**, 114818, DOI: [10.1016/j.molliq.2020.114818](https://doi.org/10.1016/j.molliq.2020.114818).

34 D. Hannachi, N. E. H. Amrane, L. Merzoud and H. Chermette, Exploring the antioxidant activity of thiaflavan compounds: a quantum chemical study, *New J. Chem.*, 2021, **45**, 13451, DOI: [10.1039/d1nj01996a](https://doi.org/10.1039/d1nj01996a).

